Heavy-quark hadroproduction in different heavy-quark mass renormalization schemes: phenomenological implications

Maria Vittoria Garzelli *in collaboration with* L. Kemmler, S.-O. Moch, O. Zenaiev

Hamburg Universität, II Institut für Theoretische Physik

mainly on the basis of arXiv:2009.07763 [hep-ph]

Workshop "Resummation, Evolution, Factorization 2020", virtual (Edinburgh), December 7 - 11, 2020

Fermion mass renormalization schemes

$*$ Fermion masses: fundamental parameters in the QCD Lagrangian. Subject to renormalization (together with the coupling constants and the fields).

$*$ Re-absorption of the UV divergences in the fermionic self-energy, by means of a renormalization procedure.

$*$ At 1-loop, for a heavy-quark with bare mass m_0 and momentum p, renormalized self-energy in dimensional regularization:

$$\begin{aligned}\Sigma^R(m_0,p,\mu) &= \frac{i\alpha_S}{4\pi}\left\{\left[\frac{1}{\epsilon}-\gamma+\ln 4\pi+A(m_0,p,\mu)\right]\not{p}\right.\\ &- \left.\left[4\left(\frac{1}{\epsilon}-\gamma+\ln 4\pi\right)+B(m_0,p,\mu)\right]m_0\right\}\\ &+ i[(Z_2-1)\not{p}-(Z_2Z_m-1)m_0]+\mathcal{O}(\alpha_S^2)\end{aligned}$$

$*$ Many options possible for the renormalization conditions:
$\Rightarrow$ different schemes for defining a heavy-quark mass.

$*$ The renormalized self-energy enters the renormalized full heavy-quark propagator:

$$S^R(p,\mu)=\frac{i}{\not{p}-m_0-i\Sigma^R(m_0,p,\mu)}$$

On-shell renormalization scheme: m^{pole}

$*$ On-shell renormalization conditions defines m^{pole} as the pole of the renormalized full fermion propagator, which can then be rewritten, order by order in perturbation theory, in terms of a denominator $(\not{p} - m^{\text{pole}})$, analogous to the denominator $(\not{p} - m_0)$ of the bare propagator.

$*$ Mass indipendent from renormalization scale.

$*$ Gauge invariant.

$*$ Widely applied in case of leptons.

$*$ Well defined in pQCD only, in case of quarks.

$*$ Based on the concept of quarks as asymptotic states (not true due to confinement!) $\Rightarrow$ The pole mass receives non-perturbative corrections in full QCD $\sim \mathcal{O}(\Lambda_{QCD}) \rightarrow$ sensitivity to long-distance physics.

Relation of $m^{\rm pole}$ to short-distance mass definitions

$$m^{\rm pole} = m^{\rm sd}(R, \mu_m) + \delta m^{\rm pole-sd}(R, \mu_m)$$

* Each short-distance mass depends on two scales:
  - R = IR scale, related to absorbing IR fluctuations into the mass
  - μ_m = UV scale
* RG evolution
* Short-distance masses are insensitive to long-distance physics: renormalon ambiguity absent! :-)
* Cross-section formulas more complicated :-(

see e.g. Hoang et al. [arXiv:0803.4214]

$\overline{\rm MS}$ renormalization scheme: $m^{\overline{\rm MS}}(\mu_m)$

* The pure term $\left(\frac{1}{\epsilon} - \gamma + \ln 4\pi\right)$ appearing in the fermionic self-energy is reabsorbed into the renormalized mass:

$$m(\mu_m) = m^0 \left\{1 + \left(\frac{\alpha_s(\mu_m)}{\pi}\right)\left[\frac{1}{\epsilon} + \ln(4\pi e^{-\gamma_E})\right]\right\} + \ldots$$

* RG evolution:

$$\mu_m^2 \frac{dm(\mu_m)}{d\mu_m^2} = -\gamma_m(\alpha_S(\mu_m))\, m(\mu_m)\,,$$

controlled by the mass anomalous dimension

$$\gamma_m(\alpha_S(\mu_m)) = \sum_{i=0}^{+\infty}\left(\gamma_i\left(\frac{\alpha_S(\mu_m)}{\pi}\right)^{i+1}\right) = \gamma_0\frac{\alpha_S(\mu_m)}{\pi} + \gamma_1\frac{\alpha_s^2(\mu_m)}{\pi^2} + \gamma_2\frac{\alpha_s^3(\mu_m)}{\pi^3} + \ldots..$$

* Coefficients γ_i presently known up $i \leq 4$.

* Possibility to set μ_m value different from m: running of $m^{\overline{\rm MS}}$ allows to resum $ln(\mu_m/m)$, advantageous for processes with $Q(\ \sim \mu_m) >> m$.

* $R{=}m^{\overline{\rm MS}}(\mu_m)$

Relation between $m^{\rm pole}$ and $m^{\overline{\rm MS}}(\mu_m)$

$*$ Considering that $m_0 = Z_m^{OS} m^{\rm pole} = Z_m^{\overline{\rm MS}}(\mu_m) m^{\overline{\rm MS}}(\mu_m)$, the relation between the masses is computed making the ratio between the renormalization factors. One gets:

$$m^{\rm pole} = m^{\overline{\rm MS}}(\mu_m) \left(1 + \sum_{i=1}^{\infty} c_i \left(\frac{\alpha_S}{\pi}\right)^i\right),$$

$*$ worked out by [Tarrach 1981, Gray at al. 1990, Chetyrkin et al. 2000, Melnikov et al. 2000, Marquard et al. 2007, 2015, 2016] at various degrees of accuracy along the years (at present, up to 4-loops).

$*$ First two coefficients:

$$\begin{aligned} c_1 &= \frac{4}{3} + L, \\ c_2 &= \frac{307}{32} + 2\zeta_2 + \frac{2}{3}\zeta_2 \ln 2 - \frac{1}{6}\zeta_3 + \frac{509}{72}L + \frac{47}{24}L^2 \\ &\quad - \left(\frac{71}{144} + \frac{1}{3}\zeta_2 + \frac{13}{36}L + \frac{1}{12}L^2\right) n_{lf} + \frac{4}{3} \sum_{1 \le i \le n_{lf}} \Delta\left(\frac{m_i}{m(\mu_m)}\right), \end{aligned}$$

with $L \equiv \ln(\mu_m^2 / m(\mu_m)^2)$.

$\overline{\mathrm{MS}}$ reference mass $m(m)$

* Particular scale μ_m^* such that $\mu_m^* = m(\mu_m^*)$ leads to the "reference" $\overline{\mathrm{MS}}$ mass $m(m) = m(\mu_m^*) = \mu_m^*$.

* $m(m)$ extracted with high precision in a number of experiments (see PDG compilation).

* Relation between m^{pole} and $m(m)$:

$$m^{\mathrm{pole}} = m(m)\left[1 + 1.333\left(\frac{\alpha_S}{\pi}\right) + (13.44 - 1.041\, n_{lf})\left(\frac{\alpha_S}{\pi}\right)^2 + (190.595 - 27.0\, n_{lf} + 0.653\, n_{lf}^2)\left(\frac{\alpha_S}{\pi}\right)^3 + \mathcal{O}(\alpha_S^4)\right],$$

  with $n_{lf} + 1$ active flavours contributing to the running of α_S.

* Decoupling relation to transform to schemes with n_{lf} active flavours.

* Asymptotically, the convergence of the perturbative series is spoiled by renormalon ambiguities! [Bigi et al. 1994, Beneke and Braun 1994, Smith and Willenbrock 1996, Beneke 1998, Beneke et al. 2016]

MSR renormalization schemes: $m^{\rm MSR}(R)$

$*$ Introduced by [Hoang, Jain, Scimemi and Stewart, PRL 101 (2008) 151602]. See also further works by Hoang et al.

$*$ R treated as a *variable*.
$\Rightarrow$ RG evolution equation with respect to R:

$$R\,\frac{dm^{\rm MSR}(R)}{dR} \;=\; -R\,\gamma^{\rm MSR}(\alpha_s(R))\,,$$

with $\gamma^{\rm MSR}(\alpha_s(R)) \equiv \sum_{i=0}^{\infty}\,\gamma_i^{\rm MSR}\,(\alpha_s(R)/\pi)^{i+1}$.

$*$ Besides reabsorbing $\left(\frac{1}{\epsilon}-\gamma+\ln 4\pi\right)$ the MSR mass reabsorbs finite corrections from scales above R, appearing in the fermionic self-energy
$\Rightarrow$ R can be chosen smaller than the mass.

$*$ $m^{\rm MSR}(R)$ nicely interpolates between $m(m)$ and $m^{\rm pole}$, to which it reduces for $R \to m(m)$ and $R \to 0$, respectively.

$\Rightarrow$ Useful for the study of observables whose mass sensitivity is affected by QCD dynamics at scales $R < m$ for which the $\overline{\rm MS}$ mass is not adequate.

Example of conversion of masses between different schemes

MSR(1)	MSR(3)	MSR(9)	$m(m)$	$m^{\rm pl}_{\rm 1lp}$	$m^{\rm pl}_{\rm 2lp}$ from $m(m)$	$m^{\rm pl}_{\rm 3lp}$	$m^{\rm pl}_{\rm 1lp}$	$m^{\rm pl}_{\rm 2lp}$ from MSR(3)	$m^{\rm pl}_{\rm 3lp}$
top-quark									
171.8	171.5	170.9	162.0	169.5	171.1	171.6	171.8	172.0	172.1
172.9	172.5	171.9	163.0	170.5	172.1	172.6	172.9	173.0	173.1
173.9	173.6	173.0	164.0	171.5	173.2	173.6	173.9	174.1	174.2
charm-quark									
1.33	0.94	0.31	1.25	1.46	1.68	1.98	1.25	1.44	1.61
1.37	0.97	0.35	1.28	1.50	1.70	2.00	1.29	1.48	1.65
1.40	1.01	0.38	1.31	1.53	1.73	2.02	1.33	1.52	1.69

$*$ Numerical values for heavy-quark MSR, $\overline{\rm MS}$ and pole masses, all in GeV. Input: $m(m)$ values, 3-loop R-evolution from the scale $R_0 = m(m)$ to R. We fix $\alpha_s(M_Z)^{n_f=5} = 0.118$ ($\alpha_s(M_Z)^{n_f=3} = 0.106$) and we evolve α_S at four loops in all cases.

$*$ Top pole mass at 2- and 3-loops similar to the $m^{\rm MSR}(m_t)$ value from which the conversion is done.

$*$ Charm pole masses obtained from the conversion of either $\overline{\rm MS}$ or MSR masses, do not seem to converge!

RG evolution of the $m^{\overline{\rm MS}}(\mu)$ and $m^{\rm MSR}(R)$ masses

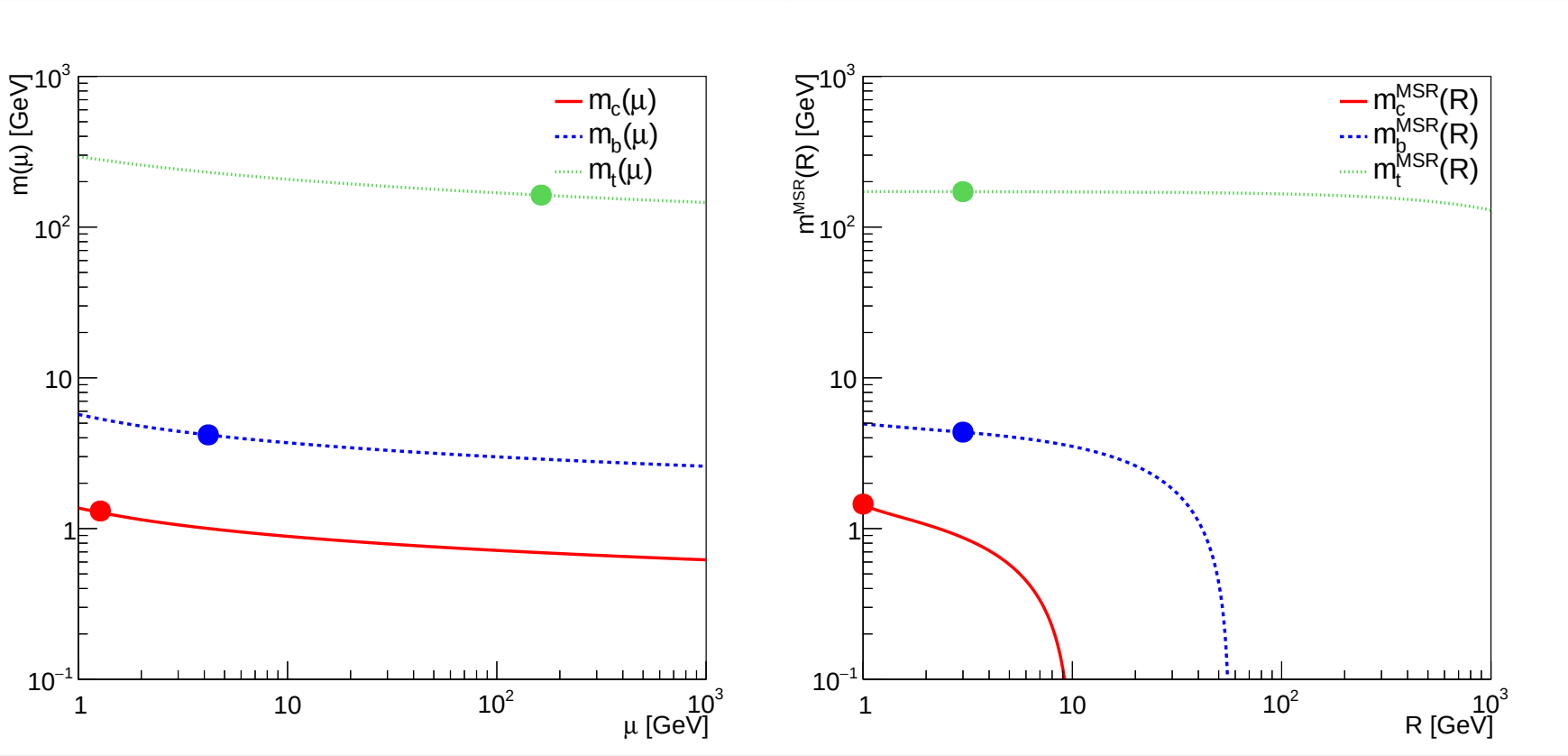

* Solution of the RG equations at 1-loop.
* Input: α_S evolution at 4-loop, with $\alpha_S(m_Z) = 0.118$, $m(m)$ values.
* $m^{\rm MSR}$ decreases with R due to the positive sign of γ_0^{MSR}.

Differential cross-sections with $\overline{\rm MS}$ and MSR heavy-quark masses

∗ Recipe: start from the cross-sections in terms of the pole mass. Perform a replacement of the pole mass with its expression in terms of short-distance masses at all orders. Expand the cross-section in α_S up to the desired order, at fixed short-distance mass value.

∗ Formulae worked out by [Langenfeld et al. 2009, Aliev et al. 2010, Dowling and Moch, 2014, Catani et al. 2020].

∗ At NLO:

$$\sigma(m(\mu_R)) = \sigma(m^{\rm pole})\Big|_{m^{\rm pole}=m(\mu_m)} + (m(\mu_m) - m^{\rm pole}) \left(\frac{\partial \sigma^{\rm Born}}{\partial m}\right)\Big|_{m^{\rm pole}=m(\mu_m)},$$

$$\sigma(m^{\rm MSR}(R)) = \sigma(m^{\rm pole})\Big|_{m^{\rm pole}=m^{\rm MSR}(R)} + (m^{\rm MSR}(R) - m^{\rm pole}) \left(\frac{\partial \sigma^{\rm Born}}{\partial m}\right)\Big|_{m^{\rm pole}=m^{\rm MSR}(R)}.$$

Differential cross-section for charm production, using $m^{\rm pole}$, $m(m)$ and $m^{\rm MSR}(R = 1\,{\rm GeV})$

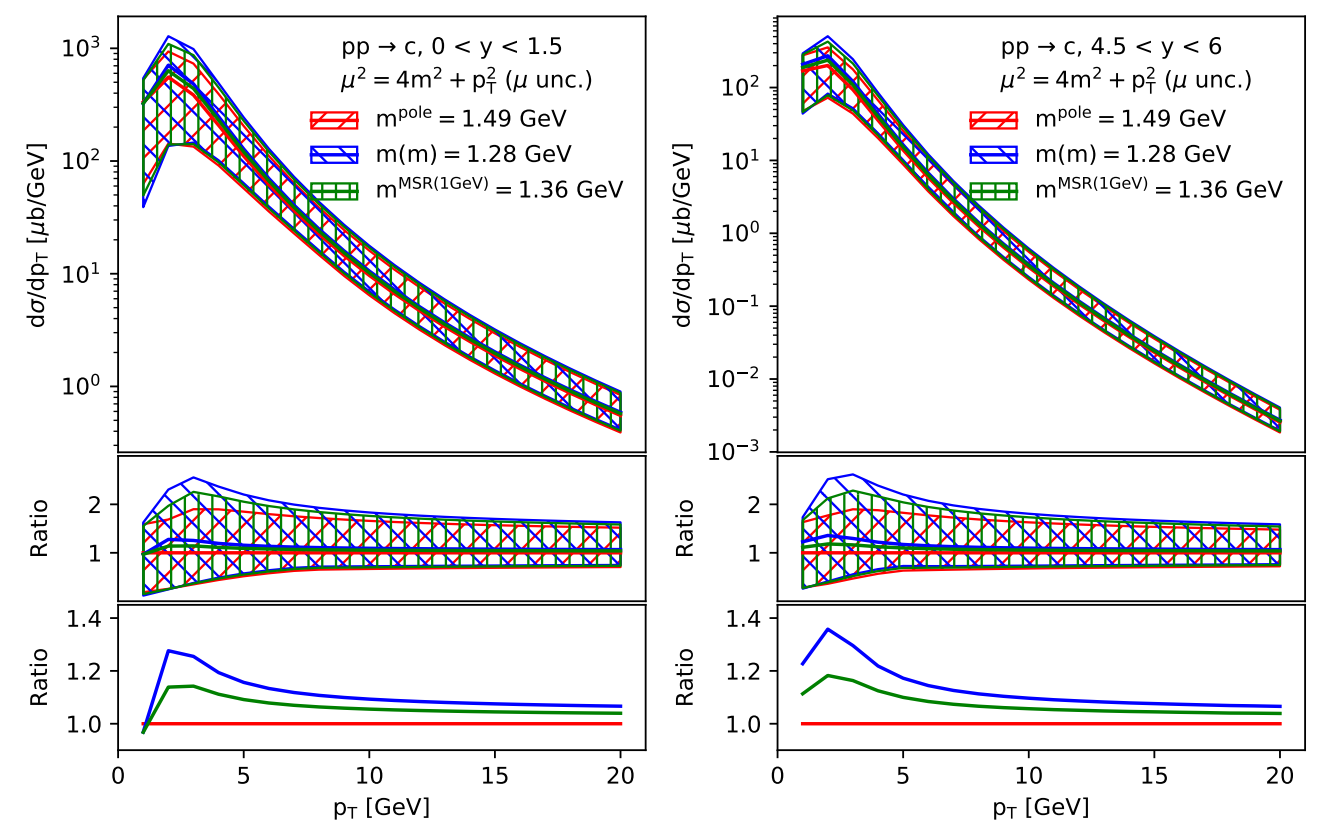

* charm p_T distribution, for various rapidity bins, at NLO, considering $pp \to c\bar{c}$ at $\sqrt{s} = 7$ TeV.
* The shape of central predictions is sensitive to the renormalization scheme: differences up to $\sim 40\%$ at the peak.
* However, size of the (μ_R, μ_F) uncertainties much larger, and of the same order of magnitude in the various mass renormalization scheme.

Differential cross-section for top production, using m^{pole}, $m(m)$ and $m^{\text{MSR}}(R = 3\,\text{GeV})$

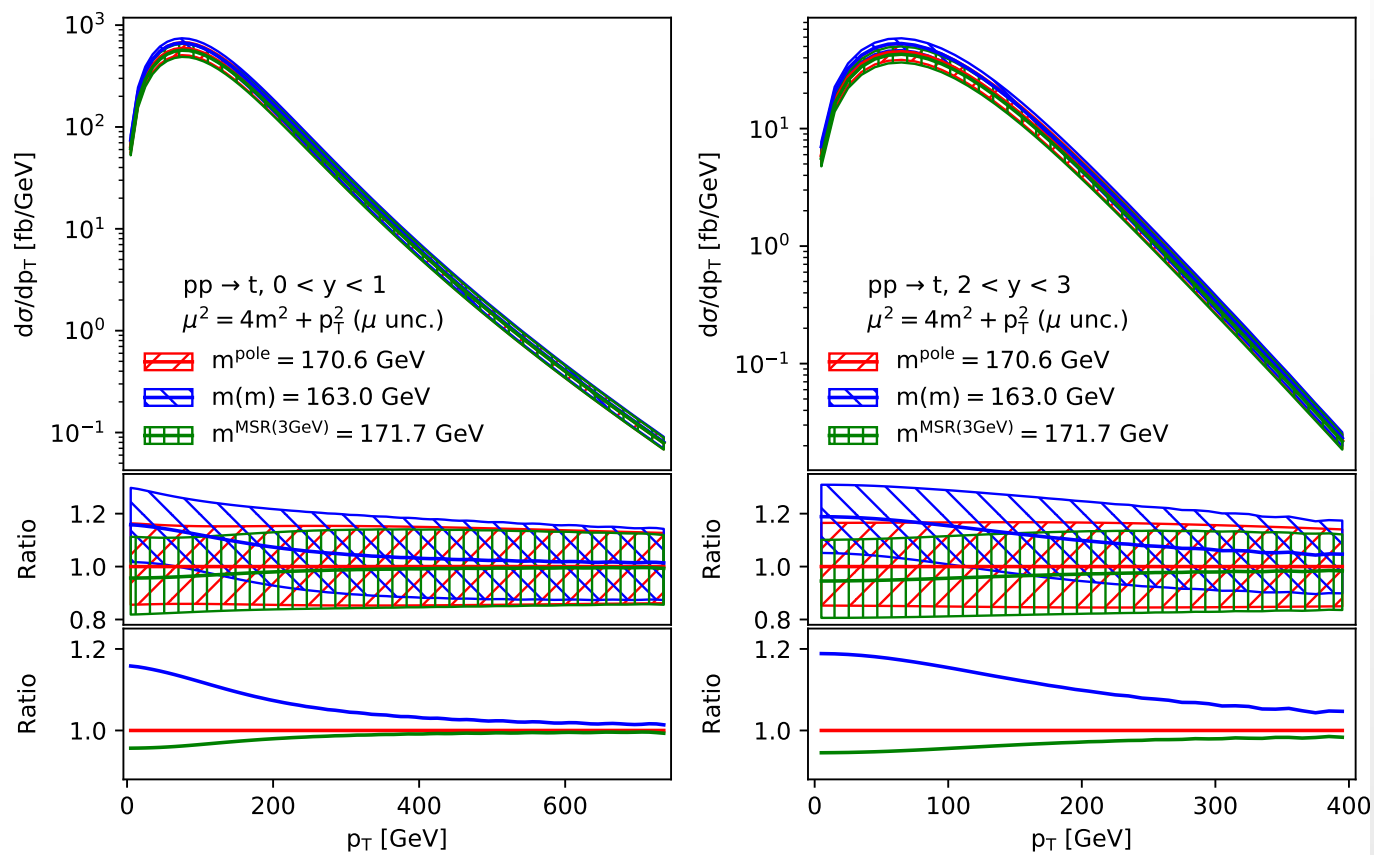

* top p_T distribution, for various rapidity bins, at NLO, considering $pp \to t\bar{t}$ at $\sqrt{s} = 7$ TeV.
* The shape of central predictions at the peak is sensitive to the renormalization scheme: differences up to $\sim 20\%$.
* Size of the (μ_R, μ_F) uncertainties of the same order of magnitude.

Mass uncertainties on $p_{T,c}$ distributions at NLO, using $m^{\rm pole}$, $m(m)$ and $m^{\rm MSR}(R = 1\,{\rm GeV})$

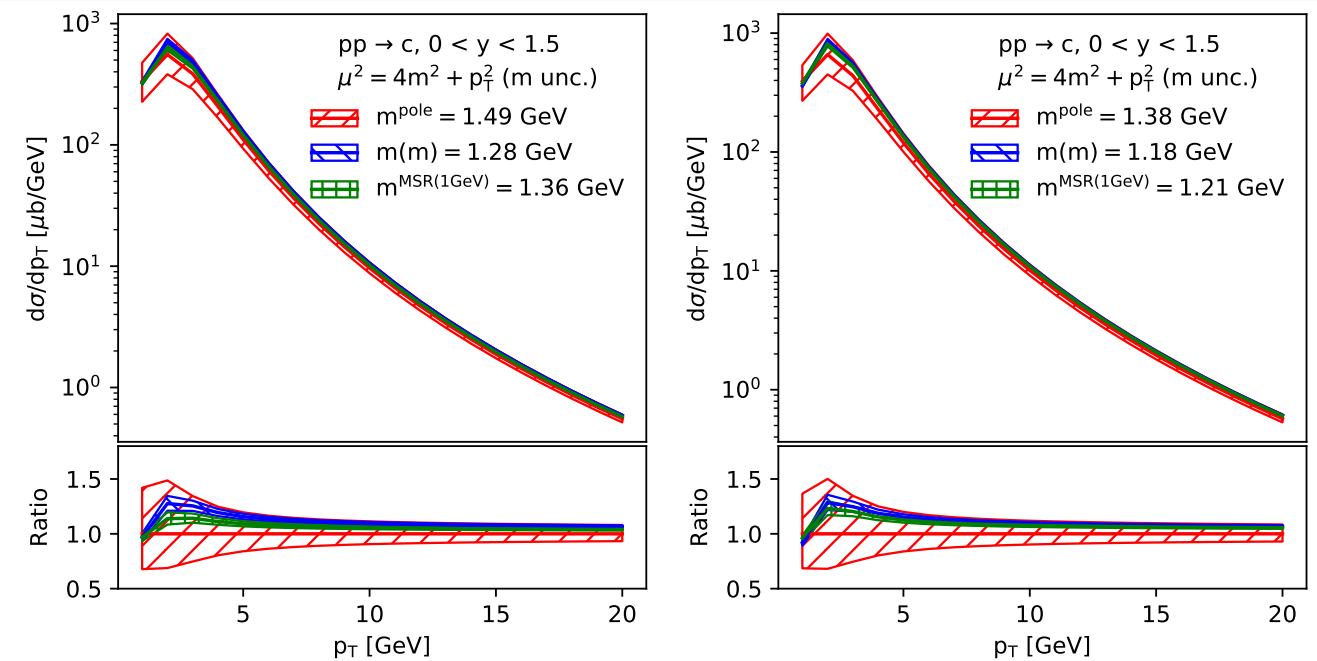

* $m_c(m_c) = 1.28 \pm 0.03$ GeV from PDG, $m_c(m_c) = 1.18 \pm 0.03$ GeV from ABMP16
* Correlations between $m_q(m_q)$, α_S and PDFs $\rightarrow$ simultaneous extraction of these quantities already performed in the framework of some PDF fits.
* Consistent use of $m_q(m_q)$, α_S and PDFs on the predictions on the right plot.
* Mass uncertainties in case of pole masses are larger, because of the renormalon ambiguity: $\Delta m^{\rm pole} \sim 0.25$ GeV assumed in these plots.
* Mass uncertainties for MSR masses as those for $m_c(m_c)$ because the coefficients in the conversion formula from $m(m)$, do not depend on the mass.

Mass uncertainties on $p_{T,b}$ distributions at NLO, using $m^{\rm pole}$, $m(m)$ and $m^{\rm MSR}(R = 3GeV)$

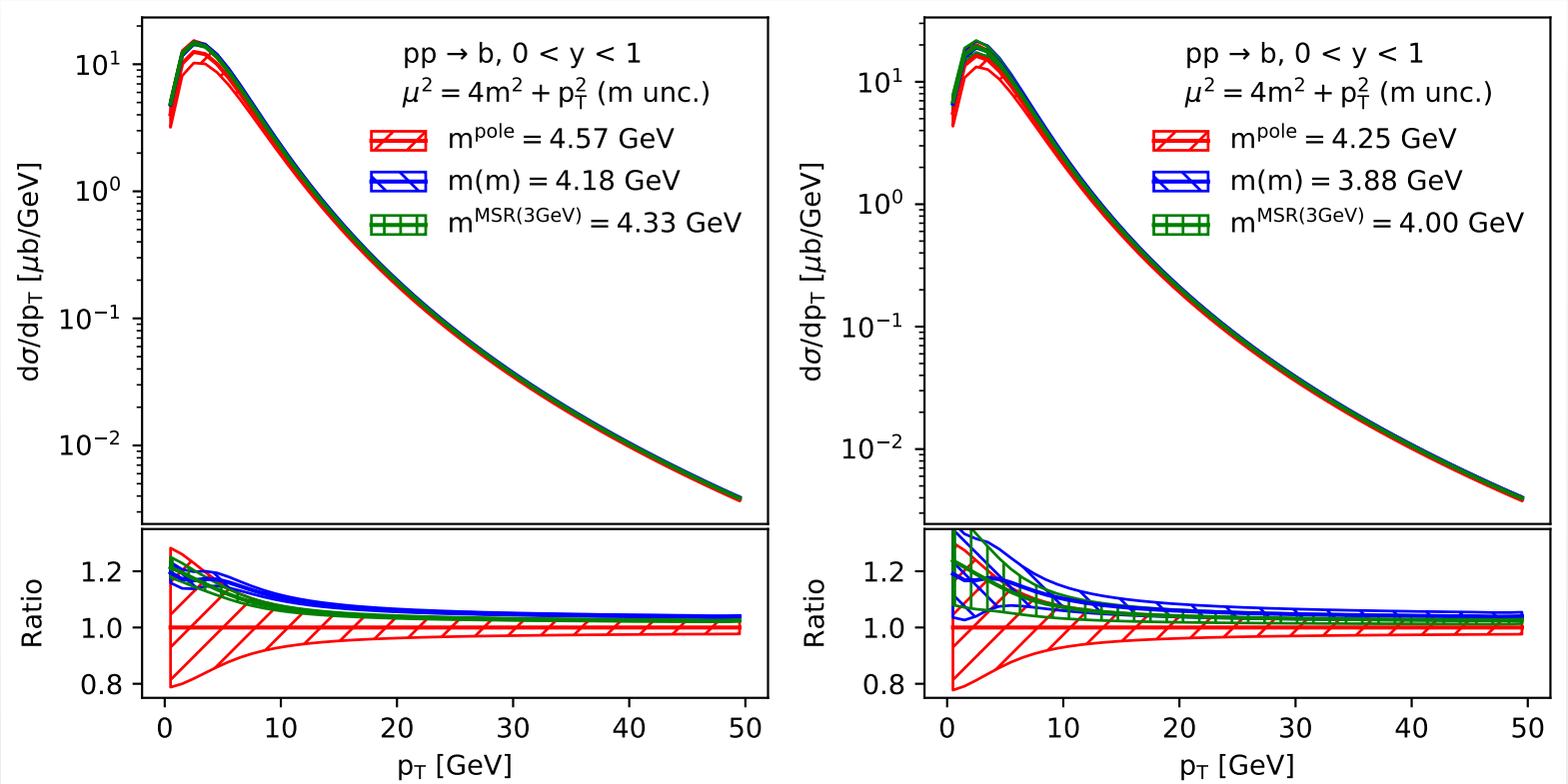

∗ $m_b(m_b) = 1.28 \pm 0.03$ GeV from PDG, $m_b(m_b) = 1.18 \pm 0.03$ GeV from ABMP16

∗ Same considerations as for the previous slide, except that the uncertainty on the bottom mass is enlarged in case of ABMP16 fit, due to the fact that bottom production in DIS is less well constrained than the charm one by the available experimental data.

$p_{T,t}$ distributions with and a dynamical vs. static mass renormalization scale

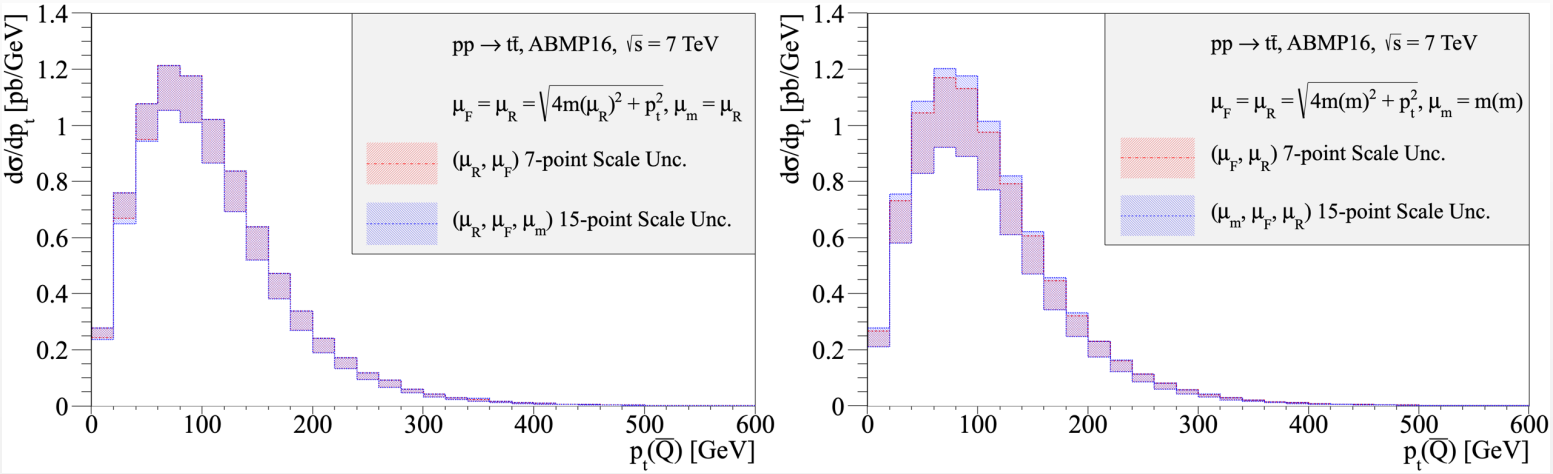

* $\mu_F^0 = \mu_R^0 = \mu_m^0 = \sqrt{p_T^2 + 4m(\mu_m^0)^2}$ vs.
  $\mu_F^0 = \mu_R^0 = \sqrt{p_T^2 + 4m(m)^2}$ and $\mu_m^0 = m(m)$.
* (μ_R, μ_F, μ_m) 15-point scale variations in intervals $(1/2,2)$ with respect to the central $(\mu_R^0, \mu_F^0, \mu_m^0)$.
* Reduced scale uncertainties in the distribution with dynamical μ_m with respect to the static case $\mu_m = m(m)$.
* Effect non visible in case of charm.

$p_{T,t}$ distributions for various (μ_R, μ_F) scales, with static $\mu_m = m(m)$

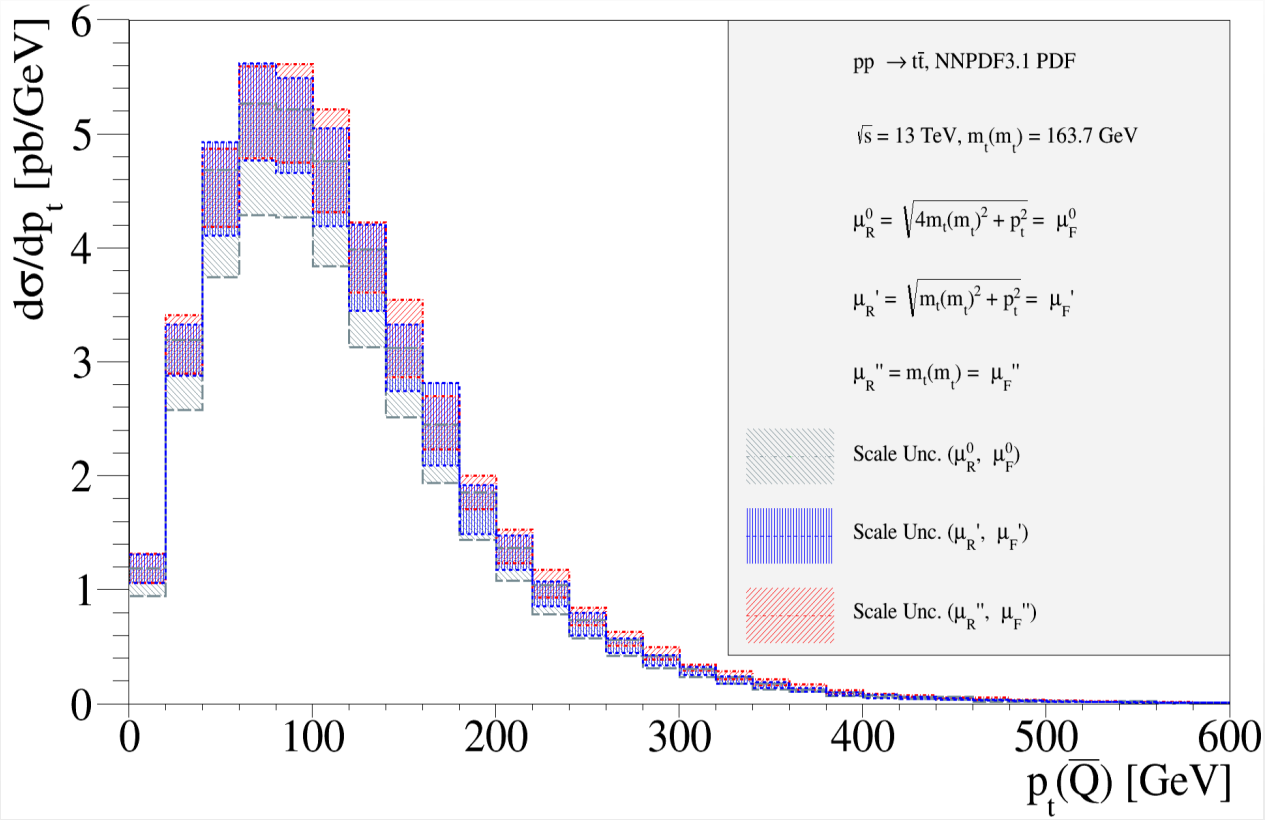

Using $(\mu_R, \mu_F) = \sqrt{p_T^2 + 4m(m)^2}$ gives rise to 7-point scale uncertainty bands larger than those obtained by using $(\mu_R, \mu_F) = \sqrt{p_T^2 + m(m)^2}$ or $(\mu_R, \mu_F)=m(m)$

$p_{T,t}$ distributions for dynamical and static mass renormalization scales

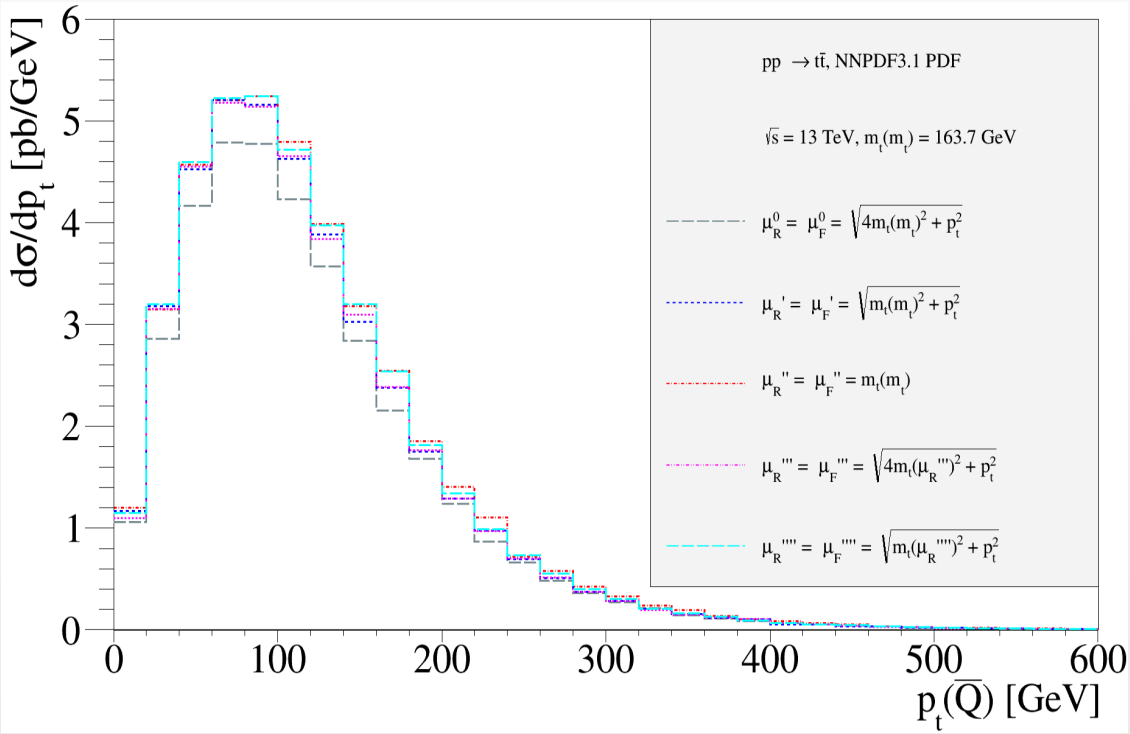

∗ Small NNLO corrections when using $\mu_F = \mu_R = m(m)$ reported by Catani et al. [arXiv:2005.00557]

∗ Predictions using $\mu_F = \mu_R = \mu_m = \sqrt{p_T^2 + m_t^2(\mu_R)}$ sit close to both the ones with $\mu_F = \mu_R = \mu_m = \sqrt{p_T^2 + m_t^2(m_t)}$ and $\mu_F = \mu_R = \mu_m = m(m)$.

∗ Predictions using $\mu_F = \mu_R = \mu_m = \sqrt{p_T^2 + 4m_t^2(\mu_R)}$ sit much closer to those with $m(m)$, than those with $\mu_F = \mu_R = \mu_m = \sqrt{p_T^2 + 4m_t^2(m_t)}$.

The "slow" perturbative convergence of this renormalization scale turns out to be improved by the use of a dynamical mass renormalization scale, instead of a static one.

Simultaneous extraction of top mass, $\alpha_S(M_z)$ and PDFs from CMS + HERA data

* CMS data on double and triple differential cross-sections reported in [arXiv:1904.05237] and H1-ZEUS combined HERA inclusive DIS data [arXiv:1506.06042] are used for this study.
* Methodology adopted similar to the one used by the CMS collaboration.
  New: extraction of the $\overline{\rm MS}$ and MSR top masses.

Settings	Fit results
pole mass	$\chi^2/\text{dof} = 1364/1151$, $\chi^2_{t\bar{t}}/\text{dof} = 20/23$
$\mu_R = \mu_F = H'$	$m_t^{\rm pole} = 170.5 \pm 0.7(\text{fit}) \pm 0.1(\text{mod})^{+0.0}_{-0.1}(\text{par}) \pm 0.3(\mu)$ GeV
Ref. CMS paper	$\alpha_S(M_Z) = 0.1135 \pm 0.0016(\text{fit})^{+0.0002}_{-0.0004}(\text{mod})^{+0.0008}_{-0.0001}(\text{par})^{+0.0011}_{-0.0005}(\mu)$
pole mass	$\chi^2/\text{dof} = 1363/1151$, $\chi^2_{t\bar{t}}/\text{dof} = 19/23$
$\mu_R = \mu_F = m_t^{\rm pole}$	$m_t^{\rm pole} = 169.9 \pm 0.7(\text{fit}) \pm 0.1(\text{mod})^{+0.0}_{-0.0}(\text{par})^{+0.3}_{-0.9}(\mu)$ GeV
our work	$\alpha_S(M_Z) = 0.1132 \pm 0.0016(\text{fit})^{+0.0003}_{-0.0004}(\text{mod})^{+0.0003}_{-0.0000}(\text{par})^{+0.0016}_{-0.0008}(\mu)$
$\overline{\rm MS}$mass	$\chi^2/\text{dof} = 1363/1151$, $\chi^2_{t\bar{t}}/\text{dof} = 19/23$
$\mu_R = \mu_F = m_t(m_t)$	$m_t(m_t) = 161.0 \pm 0.6(\text{fit}) \pm 0.1(\text{mod})^{+0.0}_{-0.0}(\text{par})^{+0.4}_{-0.8}(\mu)$ GeV
our work	$\alpha_S(M_Z) = 0.1136 \pm 0.0016(\text{fit})^{+0.0002}_{-0.0005}(\text{mod})^{+0.0002}_{-0.0001}(\text{par})^{+0.0015}_{-0.0009}(\mu)$
MSR mass, $R = 3$ GeV	$\chi^2/\text{dof} = 1363/1151$, $\chi^2_{t\bar{t}}/\text{dof} = 19/23$
$\mu_R = \mu_F = m_t^{\rm MSR}$	$m_t^{\rm MSR} = 169.6 \pm 0.7(\text{fit}) \pm 0.1(\text{mod})^{+0.0}_{-0.0}(\text{par})^{+0.3}_{-0.9}(\mu)$ GeV
our work	$\alpha_S(M_Z) = 0.1132 \pm 0.0016(\text{fit})^{+0.0003}_{-0.0004}(\text{mod})^{+0.0002}_{-0.0000}(\text{par})^{+0.0016}_{-0.0008}(\mu)$

Comparison between the results of different extractions of $m_t(m_t)$

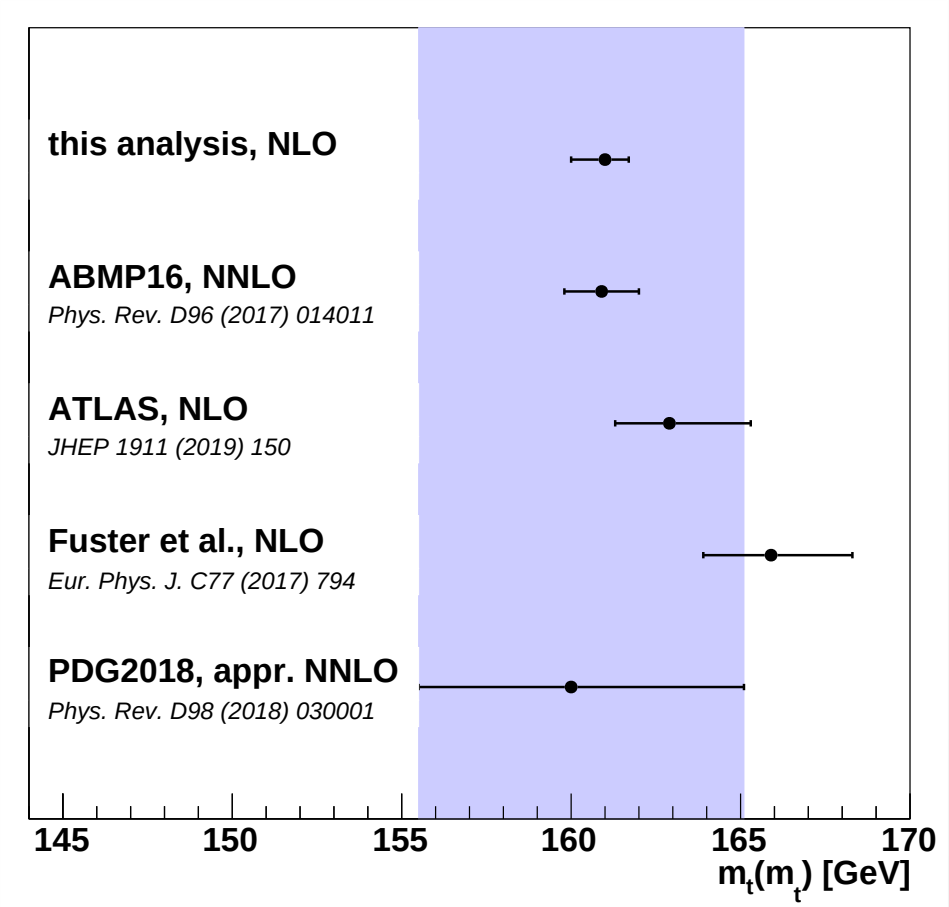

* Our results are compatible with the world average (based on a determination from the D0 collaboration).

* Only partial compatibility with the results of Fuster et al.

Total NNLO $\sigma(pp \to c\bar{c})$ for different PDF sets

compared to $\sigma_{c\bar{c}}^{TOT}$ extrapolated from LHC data

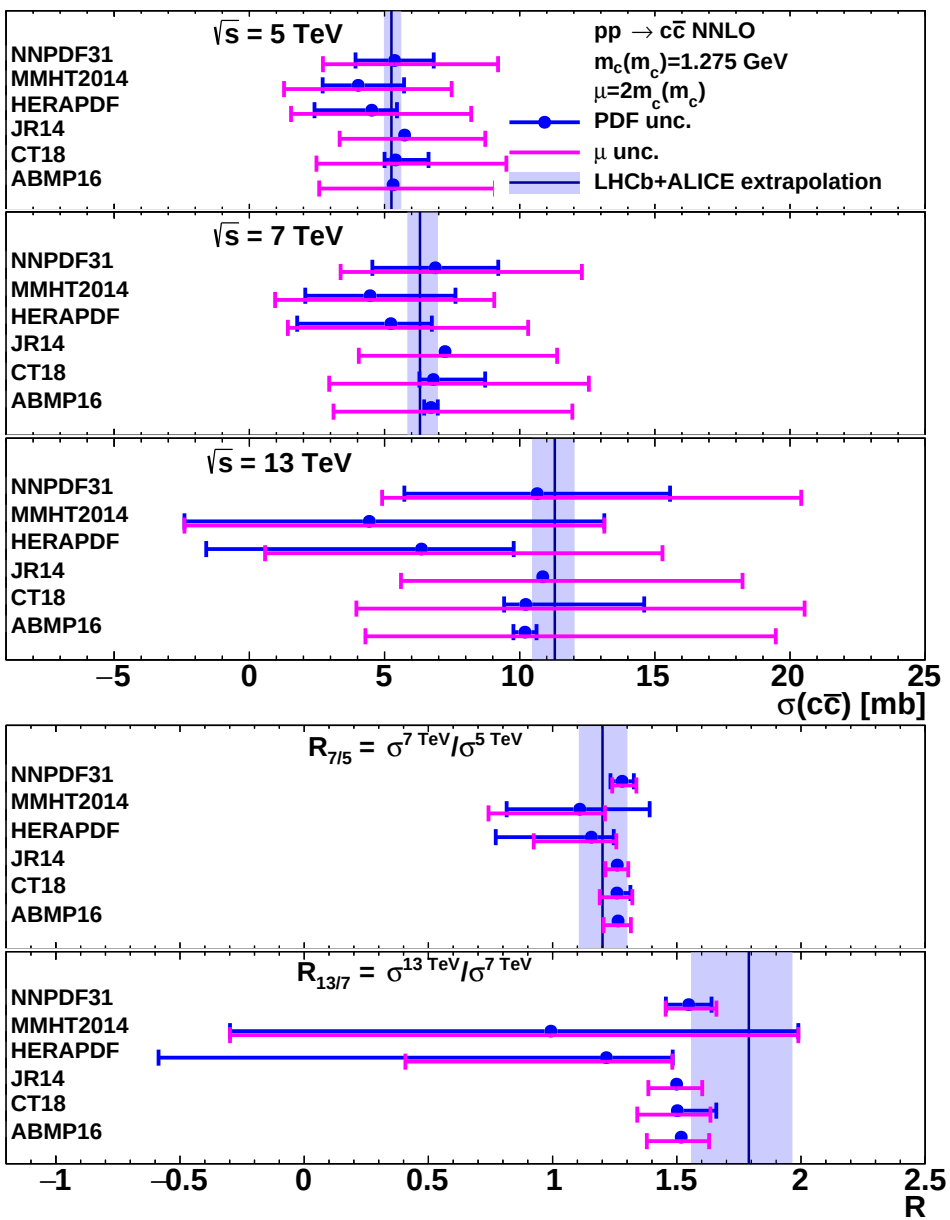

∗ Scale uncertainties larger than $\pm$ 50% even at NNLO.

∗ Size of PDF uncertainties depending on PDF fit.

∗ Consistency between different PDF sets in the values of the $R_{7/5}$ and $R_{13/7}$ ratios, within uncertainties.

from [arXiv:2009.07763]

Profiling NNLO PDFs with $R_{7/5}$ and $R_{13/7}$ built from $\sigma_{c\bar{c}}^{TOT}$

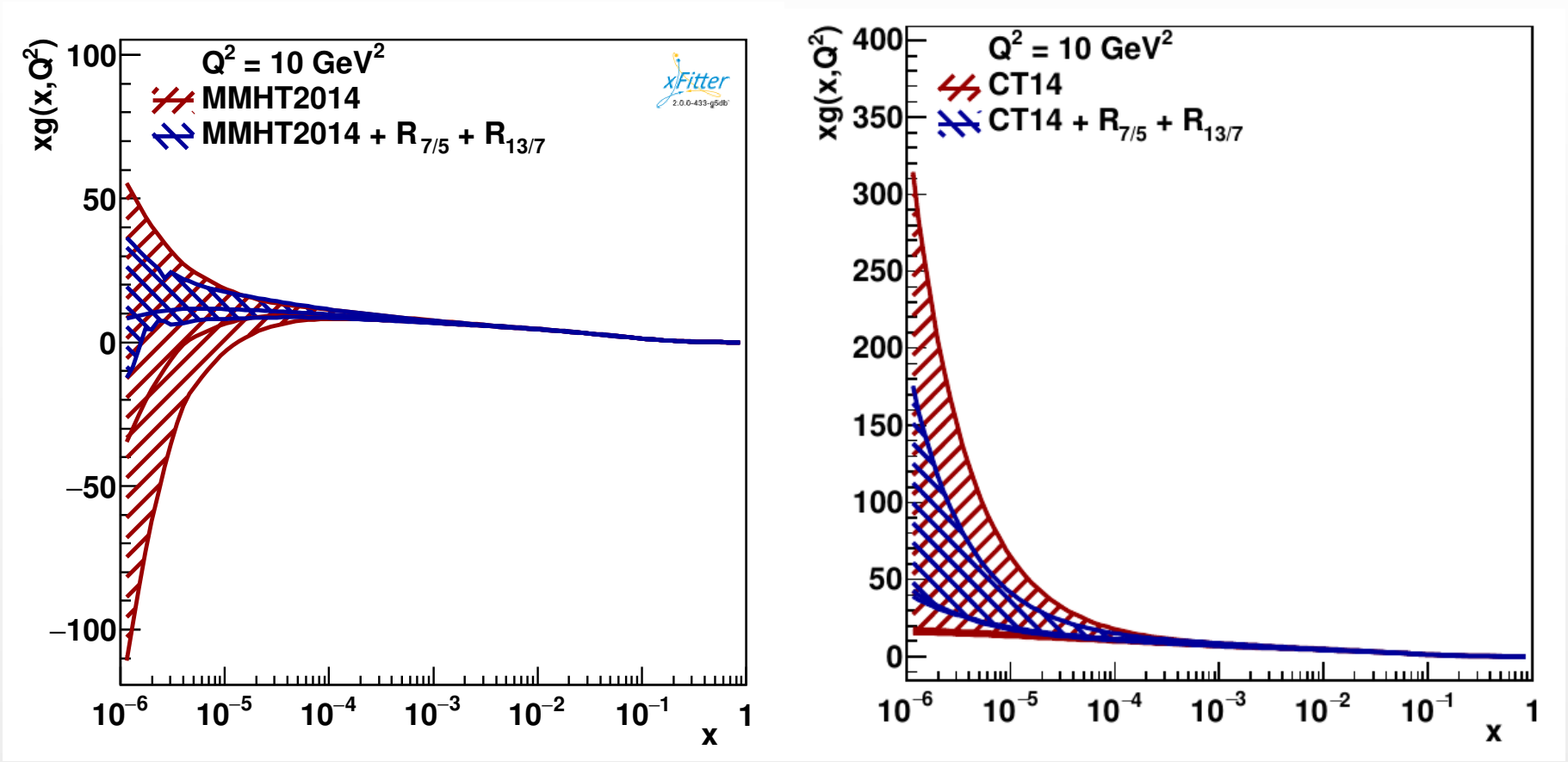

from [arXiv:2009.07763]

* Noticeable reduction of uncertainties at low x.
* Scale uncertainties effects included in the extrapolated experimental results used for this analysis, but absent in the PDF fits (:-((().

Uncertainties in the PROSA 2019 PDF fit

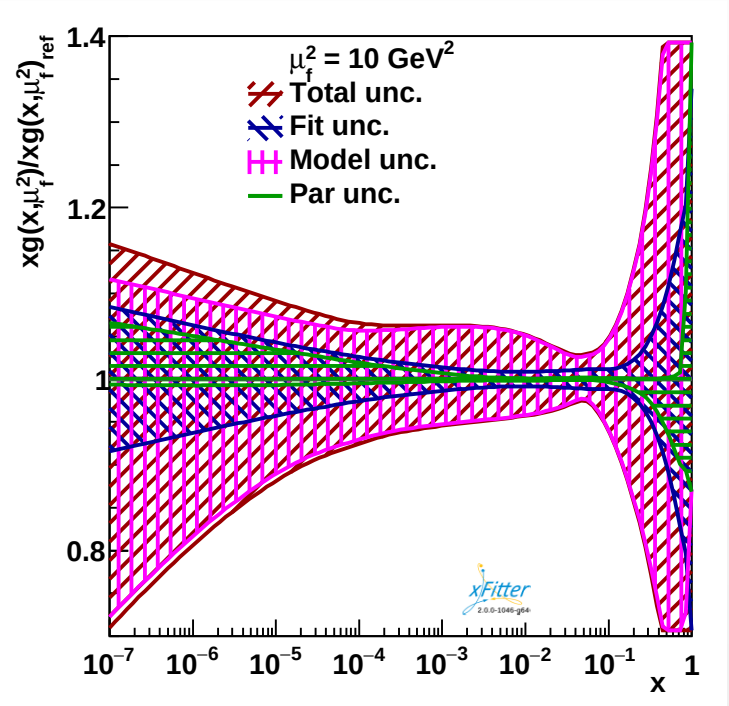

from [arXiv:1911.13164]

* Model uncertainties dominating over the others.
* for this NLO PDF fit, the uncertainty band on gluon distribution is dominated by scale uncertainties (the gluon at low x is constrained using charm data, for which scale uncertainties are very large).
* $m_c(m_c)$ fitted together with PDF, obtaining $m_c(m_c) = 1.23 \pm 0.03$ GeV.

Conclusions

$*$ Smaller parametric uncertainties when using short-distance masses with respect to $m^{\rm pole}$.

$*$ Rate of convergence of perturbative expansion for cross-sections depends on the μ_R, μ_F and μ_m scales.

$*$ Differences in cross-sections due to different mass renormalization schemes and related μ_m choices, are more marked in case of heavy (top and bottom) than for charm quark hadroproduction at the LHC (at the present accuracy).

$*$ In case of charm quark at NLO accuracy, the uncertainties related to (μ_R, μ_F) variation are much larger than those due to the use of different mass schemes. Additionally, the use of running masses can lead to $m(\mu_m) < 1$ GeV, for μ_m large enough. This can hamper the convergence of pQCD calculations.

$*$ In case of top (and bottom) production, our findings support the use of dynamical μ_m as giving faster perturbative convergence with respect to static μ_m. Further studies/investigations in this direction are under way. Further studies on optimizing R choice too.

$*$ Natural continuation of this work: extend our study to higher perturbative accuracy (NNLO, see recent work by Catani et al., and predictions with resummation of different kinds of logs).

$*$ Applications to phenomenology: simultaneous extraction/fit of PDF, α_S and m_Q in different mass renormalization schemes. The $m_Q(m_Q)$ extractions lead to values in reasonable agreement with the PDG values.